Chinese Chemical Letters 37 (2026) 111794

Contents lists available at ScienceDirect

Chinese Chemical Letters

journal homepage: www.elsevier.com/locate/cclet

Intranasal delivery of cannabidiol-loaded hypoxic exosomes for targeted treatment of methamphetamine addiction *via* enhanced brain penetration and neuroinflammation modulation

Tianshu Zhang[a,b], Xiaodong Li[c], Yinghua Peng[d,*], Cong Lin[b,*], Xiaohui Wang[a,b,*]

[a] *School of Applied Chemistry and Engineering, University of Science and Technology of China, Hefei 230026, China*
[b] *Laboratory of Chemical Biology, Changchun Institute of Applied Chemistry, Chinese Academy of Sciences, Changchun 130022, China*
[c] *Shenzhen Sciencare Drug Research Institute, Shenzhen 518118, China*
[d] *Institute of Special Animal and Plant Sciences, Chinese Academy of Agricultural Sciences, Changchun 130112, China*

ARTICLE INFO

Article history:
Received 14 June 2025
Revised 29 August 2025
Accepted 5 September 2025
Available online 5 September 2025

Keywords:
Methamphetamine addiction
Cannabidiol (CBD)
Neuroinflammation
Exosome drug delivery
Intranasal administration

ABSTRACT

Methamphetamine (METH) addiction represents a severe global public health crisis with currently limited therapeutic options, highlighting an urgent need for innovative approaches. Emerging evidence indicates that neuroinflammation, particularly microglial activation and subsequent cytokine release, significantly contributes to the neuropathology associated with METH use. Cannabidiol (CBD), a phytocannabinoid with promising anti-inflammatory and neuroprotective properties, has demonstrated therapeutic potential in mitigating METH-related neuroimmune responses. However, its clinical translation is severely restricted due to low bioavailability, rapid hepatic metabolism, and limited blood-brain barrier (BBB) penetration. To address these challenges, we developed a novel therapeutic platform utilizing exosomes derived from hypoxia-preconditioned human umbilical vein endothelial cells. These exosomes were loaded with CBD and surface-functionalized with the transcriptional activator protein (TAT) peptide, generating HP-Exo-CBD-TAT, to enhance brain targeting. Intranasal administration of HP-Exo-CBD-TAT significantly improved BBB penetration and brain accumulation compared to unmodified CBD-loaded exosomes (HP-Exo-CBD). In mouse models of METH addiction, treatment with HP-Exo-CBD-TAT markedly attenuated behavioral sensitization and conditioned place preference (CPP), two key indicators of addiction-like behaviors. The observed therapeutic effects correlated strongly with reductions in microglial activation and pro-inflammatory cytokine expression (interleukin-1β (IL-1β), IL-6, tumor necrosis factor-α (TNF-α)) in critical addiction-associated brain regions, such as the medial prefrontal cortex and ventral tegmental area. Importantly, even the carrier alone (HP-Exo-TAT) exhibited intrinsic immunomodulatory effects, underscoring the dual therapeutic action of this delivery system. Our findings highlight HP-Exo-CBD-TAT as a highly efficient, biocompatible, and non-invasive strategy that effectively targets neuroinflammation and addictive behaviors. This intranasal exosomal platform demonstrates significant translational promise for the clinical management of METH addiction.

© 2026 Published by Elsevier B.V. on behalf of Chinese Chemical Society and Institute of Materia Medica, Chinese Academy of Medical Sciences.

Methamphetamine (METH), a highly addictive psychostimulant, poses a severe and pervasive global public health crisis, affecting millions of individuals worldwide [1]. Chronic METH use leads to significant neuropsychiatric morbidity, cognitive impairment, and substantial mortality, with relapse being common even after prolonged abstinence [2]. Currently, no approved pharmacotherapies exist for METH addiction, and available treatment primarily relies on behavioral interventions, which show limited effectiveness. This therapeutic gap underscores an urgent need for innovative strategies targeting the underlying pathophysiology of METH addiction.

Emerging evidence highlights neuroinflammation, particularly mediated through activated microglia, as a critical mechanism underpinning the neuropathology associated with chronic METH exposure [3]. METH use robustly activates microglia, triggering excessive release of pro-inflammatory cytokines (*e.g.*, interleukin-1β (IL-1β), IL-6, tumor necrosis factor-α (TNF-α)), which exacerbates neuronal injury, disrupts neuron–glia crosstalk, and promotes addictive behaviors [2]. Indeed, studies using rodent models have demonstrated a direct correlation between neuroinflammatory cytokine elevation and relapse behaviors, suggesting that targeted

* Corresponding authors.
E-mail addresses: pengyinghua@caas.cn (Y. Peng), cong.lin@ciac.ac.cn (C. Lin), xiaohui.wang@ciac.ac.cn (X. Wang).

https://doi.org/10.1016/j.cclet.2025.111794
1001-8417/© 2026 Published by Elsevier B.V. on behalf of Chinese Chemical Society and Institute of Materia Medica, Chinese Academy of Medical Sciences.

anti-inflammatory interventions might effectively attenuate METH-induced neuropsychiatric deficits and reduce drug-seeking behavior [4,5].

Cannabidiol (CBD), a non-psychoactive phytocannabinoid derived from *Cannabis sativa*, emerges as a particularly promising therapeutic candidate due to its potent anti-inflammatory, neuroprotective, and immunomodulatory properties [6]. In preclinical addiction models, CBD treatment consistently reduces neuroinflammatory cytokine levels and effectively prevents drug- or stress-induced reinstatement of METH-seeking behaviors [7–9]. However, the clinical translation of CBD is significantly hindered by pharmacokinetic barriers, including poor water solubility, low (~6%) oral bioavailability due to extensive first-pass hepatic metabolism, and limited blood-brain barrier (BBB) penetration [10,11]. Consequently, achieving therapeutically relevant brain concentrations requires excessively high systemic doses, potentially increasing adverse effects and restricting clinical feasibility.

To address these pharmacokinetic challenges, exosomes—endogenous, lipid bilayer–encapsulated nanovesicles secreted by virtually all cell types—have emerged as promising advanced drug delivery vehicles [12–16]. Exosomes offer distinct advantages, including intrinsic biocompatibility, low immunogenicity, and the ability to traverse biological barriers such as the BBB [16,17]. Furthermore, exosomal delivery can markedly enhance drug bioavailability, reduce systemic toxicity, and enable targeted cargo distribution within the brain [17,18]. However, naturally derived exosomes lack active targeting capabilities and exhibit suboptimal brain accumulation when administered systemically, necessitating specific functional modifications to improve their therapeutic efficacy.

Building on this premise, we engineered a novel exosome-based therapeutic platform designed explicitly for targeted brain delivery. Exosomes loaded with CBD *via* endogenous loading strategy were harvested from hypoxia-preconditioned human umbilical vein endothelial cells (HUVECs), leveraging hypoxia's ability to enhance exosomal anti-inflammatory and regenerative potential by enriching them with stress-responsive therapeutic cargo [19–21]. Subsequently, we functionalized these hypoxic exosomes with the transcriptional activator protein (TAT), an HIV-1-derived cell-penetrating peptide extensively demonstrated to improve cellular uptake and BBB permeability [22,23]. Finally, the TAT-modified hypoxic exosomes loaded with CBD were administered intranasally, a route shown to bypass the BBB *via* direct nasal-to-brain pathways, providing rapid, efficient, and non-invasive CNS drug delivery [24].

In this study, we introduce and evaluate this innovative nanotherapeutic platform (HP-Exo-CBD-TAT) for targeted intranasal delivery of CBD in preclinical models of chronic METH exposure. We hypothesize that the enhanced brain bioavailability provided by HP-Exo-CBD-TAT will effectively attenuate neuroinflammation, modulate microglial activation, and reduce METH-induced addictive behaviors. Overall, this approach presents a promising and translationally relevant strategy to address the substantial therapeutic challenges associated with METH addiction.

To implement this strategy and establish the HP-Exo-CBD-TAT platform, careful selection of the exosomal source was critical, considering the inherent functional properties of exosomes derived from different cell conditions. Given previous evidence demonstrating enhanced anti-inflammatory properties of exosomes obtained from hypoxia-preconditioned HUVECs, we selected hypoxic HUVECs as the exosomal source. Normoxic HUVEC-derived exosomes (Exo) served as a comparative control. Additionally, to effectively load CBD into exosomes using an endogenous loading strategy, we first assessed the cytotoxicity profile of CBD under normoxic and hypoxic conditions. Cell viability assays indicated that 5 μmol/L CBD was the maximum tolerable concentration suitable for further loading studies (Fig. S1 in Supporting information). Subsequently, CBD-loaded exosomes (HP-Exo-CBD) were isolated from HUVECs cultured under hypoxic conditions in the presence of 5 μmol/L CBD *via* ultracentrifugation. To enhance brain targeting capability, these CBD-loaded hypoxic exosomes were further modified with transcriptional activator protein (TAT), generating HP-Exo-CBD-TAT. For comprehensive assessment in subsequent *in vivo* experiments, TAT-modified hypoxic exosomes without CBD loading (HP-Exo-TAT) were included as an additional control group, enabling us to distinguish the effects attributable to CBD *vs.* the carrier system itself (Fig. S2 in Supporting information).

Following the construction of the HP-Exo-CBD-TAT platform, morphological analysis by transmission electron microscope (TEM) revealed that all exosome preparations exhibited a characteristic cup- or spherical-shaped structure, confirming structural integrity post-loading and modification (Fig. S3A in Supporting information). Dynamic light scattering (DLS) measurements indicated a slight increase in particle size following CBD loading and TAT modification; the mean particle diameters for Exo, HP-Exo, HP-Exo-CBD, HP-Exo-TAT, and HP-Exo-CBD-TAT were 128.3 ± 0.5, 131.1 ± 1.4, 147.6 ± 2.0, 185.7 ± 4.9, and 186.5 ± 3.4 nm, respectively (Figs. S3B and S4A in Supporting information). Correspondingly, zeta potential measurements revealed a mild neutralization from approximately -8 mV to about -4 mV after TAT conjugation, confirming successful surface modification without substantially altering the inherent properties of exosomes (Fig. S4B in Supporting information). Total internal reflection fluorescence (TIRF)-illuminated stochastic optical reconstruction microscopy (STORM) super-resolution microscope images of HP-Exo-CBD-TAT also demonstrated the attachment of TAT to the exosomes (Fig. S4C in Supporting information). To further verify exosome sizing, we employed nanoflow cytometry, which showed mean diameters of approximately 60 nm for all preparations, consistent with typical exosomal dimensions (Fig. S3C in Supporting information). Although TEM, DLS, and nanoflow cytometry provided slightly varying absolute size values due to methodological differences, all measured exosome sizes consistently fell within the expected range of 30–200 nm. Moreover, western blot analysis confirmed the purity and identity of isolated exosomes by detecting characteristic exosome-specific markers (TSG101, Alix, CD63, CD81) while demonstrating the absence of GM130, a negative control protein indicative of cellular debris (Fig. S3D in Supporting information).

Beyond physical characterization, CBD encapsulation efficiency and loading capacity were crucial parameters determining therapeutic efficacy. High performance liquid chromatography (HPLC) analysis revealed a satisfactory loading capacity of 16.3% and an encapsulation efficiency of 7.8%. Additionally, controlled-release studies using dialysis demonstrated that CBD release from HP-Exo-CBD was gradual, reaching a cumulative release of approximately $53.3\% \pm 1.4\%$ over 24 h (Fig. S3E in Supporting information), highlighting the potential suitability of this formulation for sustained delivery applications.

After characterizing the physicochemical properties and drug release profile of our exosomal platform, we proceeded to assess its biological activity. Considering that microglial activation plays a pivotal role in neuroinflammation associated with METH abuse, we next investigated whether hypoxia-conditioned exosomes could modulate microglial polarization toward an anti-inflammatory (M2) phenotype. BV-2 microglial cells were stimulated with lipopolysaccharide (LPS) in the presence of either normoxic (Exo) or hypoxic (HP-Exo) exosomes. Quantitative reverse transcription polymerase chain reaction (qRT-PCR) analyses showed significant suppression of pro-inflammatory M1 markers, including IL-1β (Fig. 1A), inducible nitric oxide synthase (iNOS) (Fig. 1B), and IL-6 (Fig. 1C), exclusively in HP-Exo-treated cells. Concurrently, HP-Exo significantly enhanced the expression of M2 polarization markers Arg-1 (Fig. 1D) and IL-4 (Fig. 1E). These re-

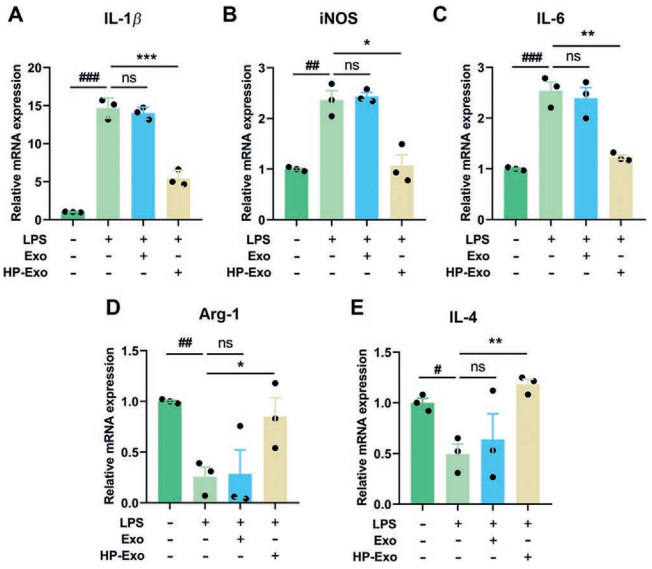


Fig. 1. Hypoxia-conditioned exosomes shifted BV-2 microglia from an M1 to an M2 phenotype after LPS challenge. BV-2 cells were treated for 6 h with LPS (20 ng/mL) alone or in combination with normoxic exosomes (Exo, 100 μg/mL) or hypoxic exosomes (HP-Exo, 100 μg/mL). Transcript levels of the pro-inflammatory M1 markers IL-1β (A), iNOS (B), and IL-6 (C) and the anti-inflammatory M2 markers Arg-1 (D) and IL-4 (E) were quantified by qRT-PCR. Data were expressed as mean ± SEM ($n = 3$ independent cultures). Statistical analysis was performed with a two-tailed unpaired Student's *t*-test. $^{\#}P < 0.05$, $^{\#\#}P < 0.01$, $^{\#\#\#}P < 0.001$ *vs.* untreated control; $^{*}P < 0.05$, $^{**}P < 0.01$, $^{***}P < 0.001$ *vs.* the LPS-only group. ns, not significant.

sults collectively indicated that hypoxia-derived exosomes inherently possess robust anti-inflammatory effects and actively promote microglial transition toward an M2 phenotype, providing a therapeutic rationale for their use in combating neuroinflammation *in vivo*.

To evaluate the efficiency of brain targeting conferred by TAT modification, we investigated the biodistribution profiles of DiD-labeled HP-Exo-CBD-TAT compared to unmodified HP-Exo-CBD following intranasal administration in nude mice. All the animal-handling procedures were approved by the Institutional Animal Care and Use Committee of Changchun Institute of Applied Chemistry, Chinese Academy of Sciences (protocol No. CIAC2022-0055). Time-course fluorescence imaging demonstrated significantly enhanced brain accumulation for HP-Exo-CBD-TAT at multiple time points, peaking around 12 h post-administration. Quantitative analysis revealed approximately 1.4- to 1.6-fold higher brain fluorescence intensity for TAT-modified exosomes relative to the unmodified group (Figs. 2A and B). Although fluorescence intensity declined in both groups by 24 h, HP-Exo-CBD-TAT maintained significantly greater residual brain localization. *Ex vivo* organ imaging corroborated these observations, confirming enhanced selective accumulation of TAT-modified exosomes in brain tissues *vs.* peripheral organs (heart, lung, liver, kidney, and spleen) (Fig. 2C). Control experiments using DiD in phosphate buffered saline (PBS) or equal CBD-containing DiD solution alone produced negligible fluorescence signals, confirming that specific brain targeting requires both TAT functionalization and intranasal administration.

With evidence of enhanced brain targeting, we next evaluated the therapeutic efficacy of our engineered exosomal system *in vivo*. We subsequently examined the therapeutic efficacy of our engineered exosomal system in a mouse model of METH-induced behavioral sensitization, characterized by progressively increased locomotor activity following repeated psychostimulant exposure (Fig. 3A). Administration of intranasal HP-Exo-CBD-TAT (2 mg/kg) significantly attenuated the development of behavioral sensitization induced by daily METH injections (1 mg/kg). Notably, this

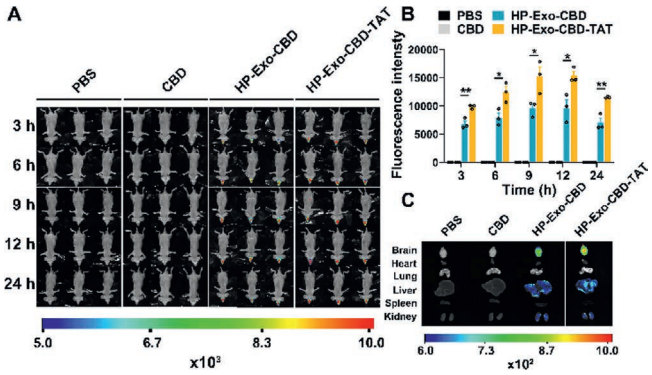


Fig. 2. TAT functionalization markedly enhanced brain accumulation of CBD-loaded exosomes after intranasal delivery. (A) Whole-body near-infrared fluorescence images recorded at 3, 6, 9, 12, and 24 h after a single intranasal dose (30 μL) of DiD-labelled HP-Exo-CBD or HP-Exo-CBD-TAT in nude mice. PBS containing DiD and CBD solution containing DiD (at an equivalent CBD dose) were included as controls. (B) Semi-quantitative analysis of mean fluorescence intensity within a cranial region of interest (ROI) at each time point (mean ± SEM, $n = 3$). TAT modification yielded a ~1.4–1.6-fold increase in brain signal relative to the non-targeted formulation. (C) *Ex-vivo* fluorescence imaging of major organs harvested 24 h post-administration confirmed preferential brain localization of HP-Exo-CBD-TAT with minimal off-target uptake. Statistical analysis: two-tailed unpaired Student's *t*-test. $^{*}P < 0.05$, $^{**}P < 0.01$ *vs.* HP-Exo-CBD.

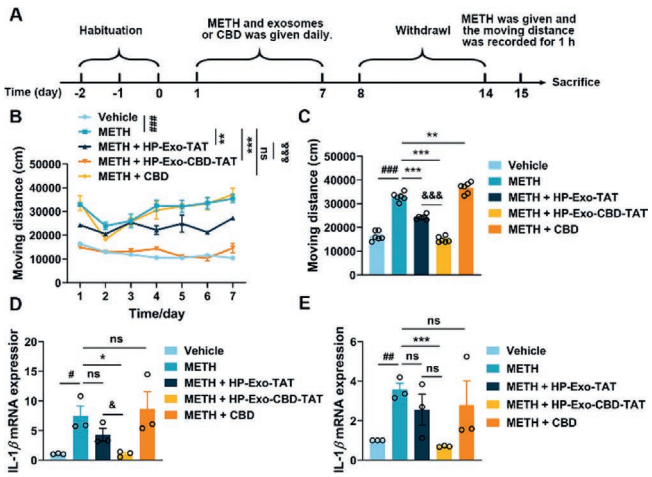


Fig. 3. Intranasal HP-Exo-CBD-TAT suppressed methamphetamine-induced locomotor sensitization and neuroinflammation. (A) Experimental timeline: mice received daily methamphetamine (METH; 1 mg/kg, intraperitoneal (i.p.)) for 7 days to induce behavioral sensitization, together with intranasal (i.n.) HP-Exo-TAT or HP-Exo-CBD-TAT (2 mg/kg) or i.p. free CBD (2 mg/kg). After a 7-day withdrawal, a METH challenge (1 mg/kg) was administered. (B) Induction phase: cumulative locomotor distance (mean ± SEM, $n = 6$) showed progressive hyperactivity in the METH group; HP-Exo-CBD-TAT completely abolished this escalation, HP-Exo-TAT produced partial attenuation, and free CBD was ineffective. (C) Challenge day: locomotor response to the single METH injection mirrored the induction results, confirming sustained protection by HP-Exo-CBD-TAT. (D, E) qRT-PCR analysis after the challenge revealed that HP-Exo-CBD-TAT normalizes IL-1β mRNA in the mPFC (D) and VTA (E) ($n = 3$), whereas HP-Exo-TAT conferred intermediate benefit. Statistics: panel B, paired two-tailed *t*-test; panels C–E, unpaired two-tailed *t*-test. $^{\#}P < 0.05$, $^{\#\#}P < 0.01$, $^{\#\#\#}P < 0.001$ *vs.* vehicle; $^{*}P < 0.05$, $^{**}P < 0.01$, $^{***}P < 0.001$ *vs.* METH; $^{\&}P < 0.05$, $^{\&\&\&}P < 0.001$ *vs.* METH + HP-Exo-TAT.

inhibitory effect was substantially more pronounced than that observed with HP-Exo-TAT alone, highlighting a critical role for CBD delivery in therapeutic efficacy. Conversely, CBD administered intraperitoneally at an equivalent dose did not alter sensitization development (Fig. 3B). Upon re-challenge with METH after a one-week withdrawal period, both HP-Exo-TAT and HP-Exo-CBD-TAT effectively mitigated hyperlocomotion, further confirming their sustained therapeutic potential (Fig. 3C).

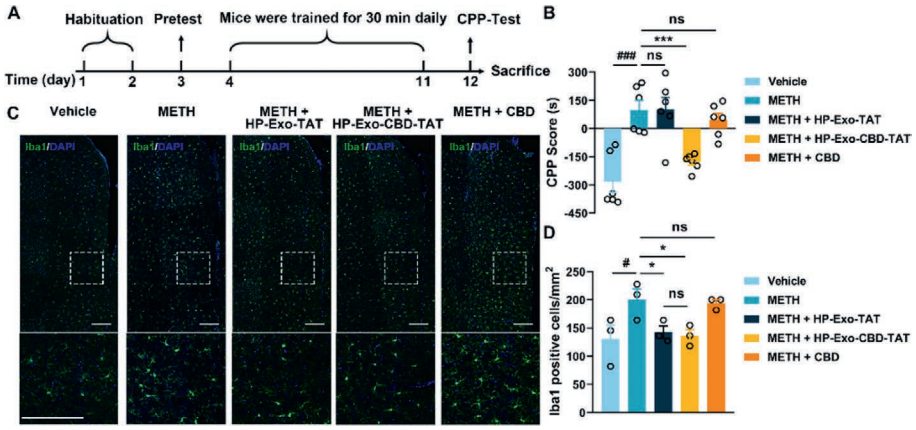


Fig. 4. HP-Exo-CBD-TAT abolished methamphetamine-induced CPP and dampened microglial activation in the mPFC region. (A) Timeline of the 12-day CPP protocol. After pre-conditioning, mice received alternate injections of methamphetamine (METH, 2 mg/kg, i.p.) or saline for four conditioning cycles; test agents—vehicle, HP-Exo-TAT (2 mg/kg i.n.), HP-Exo-CBD-TAT (2 mg/kg i.n.), or free CBD (2 mg/kg i.p.)—were given 30 min before each conditioning session. (B) CPP scores (mean ± SEM, $n = 6$). HP-Exo-CBD-TAT fully prevented METH preference, whereas HP-Exo-TAT imparted partial protection and systemic CBD was ineffective. (C) Iba1 immunofluorescence images illustrating microglial status in mPFC across treatment groups. Scale bar: 200 μm. (D) Quantification of Iba1-positive cells (cells/mm^2) in mPFC corroborated that HP-Exo-CBD-TAT normalized microglial density to control levels (mean ± SEM, $n = 3$). Statistics: panel B, unpaired two-tailed Student's *t*-test; panel D, unpaired one-tailed Student's *t*-test. $^{\#}P < 0.05$, $^{\#\#\#}P < 0.001$ *vs.* vehicle; $^{*}P < 0.05$, $^{***}P < 0.001$ *vs.* METH.

Consistent with behavioral findings, biochemical analyses demonstrated marked suppression of METH-induced pro-inflammatory cytokine IL-1β expression in critical brain regions involved in addiction pathology, namely the medial prefrontal cortex (mPFC, Fig. 3D) and ventral tegmental area (VTA, Fig. 3E). Treatment with HP-Exo-CBD-TAT normalized cytokine levels to baseline, whereas HP-Exo-TAT exhibited intermediate efficacy, correlating with its intrinsic anti-inflammatory properties previously observed *in vitro*.

Finally, to validate therapeutic potential in the context of reward-associated behavior, we employed a conditioned place preference (CPP) model of METH addiction (Fig. 4A). Mice displayed significant CPP following repeated METH pairings; however, intranasal HP-Exo-CBD-TAT treatment markedly reduced CPP scores, indicative of reduced drug reward. In contrast, neither HP-Exo-TAT nor systemic CBD alone significantly altered CPP outcomes (Fig. 4B).

Complementing behavioral data, immunofluorescence staining for microglial marker Iba1 confirmed reduced microglial activation in the mPFC (Figs. 4C and D) and VTA (Figs. S5A and B in Supporting information) following treatment with HP-Exo-CBD-TAT. Importantly, exosomes were visibly colocalized within microglia, further supporting direct therapeutic targeting of these immune cells in the CNS (Fig. S6 in Supporting information).

Overall, these findings demonstrate the robust therapeutic efficacy and superior brain targeting capability of intranasally delivered, TAT-functionalized, CBD-loaded hypoxic exosomes (HP-Exo-CBD-TAT). This advanced nanotherapeutic platform effectively mitigates neuroinflammation and behavioral pathology associated with METH addiction, underscoring its translational promise.

Alongside efficacy, the biosafety of HP-Exo-CBD-TAT was evaluated based on changes in body weight during the experiments and histological analysis of major organs. Initially, body weights were comparable across all groups: vehicle, METH, METH + HP-Exo-TAT (i.n.), METH + HP-Exo-CBD-TAT (i.n.), and METH + CBD (i.p.) (Fig. S7A in Supporting information). By day 12 (after 8 days of administration), mice in the vehicle group showed significant weight gain compared to day 1, reflecting normal growth. In contrast, the METH group exhibited significant weight loss compared to the vehicle group, indicative of METH-induced toxicity. Importantly, mice in the METH + HP-Exo-TAT (i.n.) and METH + HP-Exo-CBD-TAT (i.n.) groups did not show significant weight changes relative to the vehicle group, suggesting that intranasal administration of these formulations did not induce systemic toxicity and mitigated METH-induced weight loss. Conversely, mice in the METH + CBD (i.p.) group exhibited decreased body weight, indicating that intraperitoneal CBD administration did not effectively counteract METH-induced toxicity.

To further evaluate potential organ toxicity, liver and kidney tissues were collected from vehicle, METH, and METH + HP-Exo-CBD-TAT (i.n.) groups after behavioral testing. Histopathological analysis showed no significant pathological changes in the livers of the vehicle group. In contrast, the METH group exhibited clear necrotic foci in the liver, while these lesions were markedly reduced in the METH + HP-Exo-CBD-TAT group, suggesting a protective effect. No significant lesions were observed in the kidneys of any group, and the cortical and medullary architecture remained intact (Figs. S7B and C in Supporting information).

Overall, these findings confirm that HP-Exo-CBD-TAT demonstrates good biosafety, with no evident hepatic or renal toxicity in mice.

Building upon the demonstrated therapeutic efficacy and favorable safety profile of HP-Exo-CBD-TAT, we contextualize these findings within the broader challenge of METH addiction. METH addiction continues to present significant challenges to global public health, driven by complex neuropathological processes, particularly neuroinflammation [2]. Chronic METH exposure induces neurotoxicity primarily *via* disruptions in dopaminergic and glutamatergic signaling, oxidative stress, and metabolic disturbances, which collectively cause sustained neuronal injury [4,25]. Critically, these processes are exacerbated by activated microglia, which secrete pro-inflammatory cytokines, establishing a self-perpetuating cycle of neuroimmune dysregulation that reinforces addiction-related behaviors. Targeting this inflammatory cascade thus represents a promising therapeutic strategy to mitigate METH addiction.

CBD has emerged as a particularly compelling therapeutic candidate due to its documented anti-inflammatory, neuroprotective, and anti-addictive effects [6,8]. Despite promising preclinical outcomes, its clinical translation is severely constrained by pharmacokinetic limitations, such as poor bioavailability, rapid metabolism, and insufficient penetration of the BBB [10,11]. Consequently, advanced drug delivery approaches are necessary to realize CBD's therapeutic potential fully. Exosomes represent an attractive solution to this problem, given their inherent biocompatibility,

minimal immunogenicity, and capacity to traverse biological barriers, including the BBB [17,18]. Nevertheless, native exosomes lack intrinsic targeting specificity, limiting their efficacy as CNS therapeutics when administered systemically.

To overcome these limitations, we developed a specialized nanotherapeutic system utilizing exosomes derived from hypoxia-preconditioned HUVECs. Hypoxic preconditioning significantly enhances the exosomes' intrinsic anti-inflammatory and immunomodulatory effects [19–21], a finding corroborated by our *in vitro* studies showing their ability to shift microglial polarization toward an anti-inflammatory M2 phenotype. Furthermore, we modified these exosomes by functionalizing their surface with the cell-penetrating peptide TAT, capitalizing on its proven efficacy in facilitating mucosal permeability and improving direct CNS uptake *via* intranasal delivery [26–28]. This targeted functionalization not only circumvented systemic circulation barriers but also maximized localized brain accumulation, greatly enhancing therapeutic efficiency.

Our *in vivo* results demonstrated the therapeutic efficacy of intranasally administered TAT-modified, CBD-loaded exosomes (HP-Exo-CBD-TAT) in two established animal models of METH addiction, behavioral sensitization and CPP. Specifically, HP-Exo-CBD-TAT treatment significantly reduced both METH-induced hyperlocomotion and preference for drug-associated environments. These behavioral improvements correlated directly with marked reductions in microglial activation and normalization of pro-inflammatory cytokine profiles, particularly IL-1β, IL-6, and TNF-α, in critical regions implicated in addiction pathology, including the mPFC and VTA. Intriguingly, even the CBD-free, TAT-modified exosomes exhibited moderate anti-inflammatory and behavioral benefits, highlighting the intrinsic therapeutic potential of hypoxia-derived exosomes themselves. However, the addition of CBD notably augmented these beneficial effects, suggesting synergistic interactions between the exosomal carrier and CBD's multimodal pharmacological actions.

An essential component underlying the enhanced therapeutic outcome was the efficient brain targeting facilitated by TAT peptide conjugation and intranasal administration. Fluorescence imaging data provided direct evidence that TAT-exosomes rapidly and preferentially accumulated in the CNS following nasal administration, confirming the utility of TAT for overcoming mucosal and endothelial barriers [26]. These observations align closely with prior reports demonstrating successful CNS delivery of cell-penetrating peptide-modified nanoparticles [26,27,29]. Our results also indicated that exosomal CBD not only suppressed inflammatory microglial activation but actively promoted a beneficial shift toward anti-inflammatory phenotypes (M2 polarization). This therapeutic reprogramming of microglial responses likely stems from both the immunomodulatory effects of CBD and the intrinsic regenerative signals carried within hypoxia-conditioned exosomes, potentially including microRNAs or protective proteins [19–21]. Future studies aimed at characterizing these specific exosomal cargoes could further enhance the therapeutic potential of this delivery platform. Compared to conventional synthetic nanocarriers, our naturally derived exosome-based platform offers several substantial advantages, including reduced toxicity, minimal immunogenicity, inherent biocompatibility, and favorable scalability prospects. Previous studies have reported that synthetic peptide-functionalized nanoparticles often face challenges such as immunogenicity, rapid clearance, or insufficient BBB penetration [18]. By contrast, the exosomal formulation utilized here demonstrated a safe profile, with animals tolerating repeated intranasal administrations without observable adverse effects. Moreover, our approach achieved significantly improved therapeutic outcomes at considerably lower doses compared to systemic administration of free CBD, emphasizing the efficiency and clinical translatability of exosome-based therapies.

Despite these promising findings, several considerations and limitations remain. First, scalable and reproducible production methods must be further refined to facilitate clinical translation. Current exosome yields from cell culture are relatively limited, necessitating development of optimized bioprocessing and purification techniques. Second, the immunogenicity of exosomes derived from allogeneic cells (such as HUVECs) or modified with peptides (like TAT) warrants careful evaluation, especially for chronic or repeated dosing. Strategies such as employing autologous or genetically engineered cells producing less immunogenic exosomes may mitigate these concerns. Third, the present study focused on short-term outcomes in acute treatment paradigms; thus, long-term efficacy, safety, and dose-response relationships must be further explored in chronic addiction models, such as voluntary METH self-administration paradigms. Fourth, given CBD's poor water solubility and the requirement to preserve exosomal structural integrity, the passive loading method employed in this study, where cells are co-cultured with CBD to naturally encapsulate the drug into exosomes during biogenesis, offers operational simplicity while maintaining vesicle integrity. Nevertheless, its lower drug loading efficiency compared to active loading techniques may constrain translational applications. Finally, elucidating the precise molecular mechanisms and identifying critical exosomal cargo components responsible for the observed neuroprotective and anti-inflammatory effects will inform the rational design of next-generation therapeutic exosomes.

In summary, our study demonstrates a novel and highly promising therapeutic strategy combining targeted nanotechnology, neuroimmune modulation, and intranasal delivery to effectively address the neuroinflammatory mechanisms underlying methamphetamine addiction. The successful therapeutic outcomes achieved with the TAT-functionalized, CBD-loaded exosomal platform represent a significant advance in addiction medicine. By attenuating central neuroinflammation and interrupting pathological neural feedback loops associated with relapse, this exosome-based therapy could substantially enhance clinical interventions for METH use disorder. Future research aimed at optimizing exosome cargoes, ensuring safety, refining manufacturing processes, and conducting rigorous clinical evaluations will be crucial steps in translating this innovative nanotherapeutic approach into a transformative addition to existing addiction treatment strategies.

Declaration of competing interest

The authors declare that they have no known competing financial interests or personal relationships that could have appeared to influence the work reported in this paper.

CRediT authorship contribution statement

Tianshu Zhang: Writing – original draft, Project administration, Methodology, Formal analysis, Data curation. **Xiaodong Li:** Writing – review & editing. **Yinghua Peng:** Supervision. **Cong Lin:** Methodology. **Xiaohui Wang:** Writing – review & editing, Conceptualization.

Acknowledgments

This work was supported by the STI2030-Major Projects (No. 2021ZD0203000 (2021ZD0203003)), the National Natural Science Foundation of China (No. 22207105), the Science and Technology Innovation Program of the Chinese Academy of Agricultural Sciences (No. CAAS-ASTIP-2021-ISAPS), and the International Partnership Program of the Chinese Academy of Sciences (No. 029GJHZ2024057GC).

Supplementary materials

Supplementary material associated with this article can be found, in the online version, at doi:10.1016/j.cclet.2025.111794.

References

[1] UNODC, United Nations (2024). https://www.unodc.org/unodc/data-and-analysis/world-drug-report-2024.html.
[2] S. Shi, T. Chen, M. Zhao, Neurochem. Res. 47 (2022) 872–884.
[3] H. Li, L.R. Watkins, X. Wang, Mol. Psychiatry 29 (2024) 1912–1924.
[4] M.J. LaVoie, J.P. Card, T.G. Hastings, Exp. Neurol. 187 (2004) 47–57.
[5] D.M. Thomas, P.D. Walker, J.A. Benjamins, et al., J. Pharmacol. Exp. Ther. 311 (2004) 1–7.
[6] C. Calpe-Lopez, M.P. Garcia-Pardo, M.A. Aguilar, Molecules 24 (2019) 2583.
[7] A. Sharifi, S. Karimi-Haghighi, R. Shabani, et al., Prog. Neuropsychopharmacol. Biol. Psychiatry 113 (2022) 110458.
[8] S. Karimi-Haghighi, L. Dargahi, A. Haghparast, Addict. Biol. 25 (2020) 12740.
[9] P.H. Gobira, L.R. Vilela, B.D. Goncalves, et al., Neurotoxicology 50 (2015) 116–121.
[10] T.S. Reddy, R. Zomer, N. Mantri, Phytother. Res. 37 (2023) 1526–1538.
[11] J. Gingrich, S. Choudhuri, P. Cournoyer, et al., Food Chem. Toxicol. 176 (2023) 113799.
[12] Y. Zhang, L. Qiu, H. Li, et al., Chin. Chem. Lett. 36 (2025) 110658.
[13] Y. Xu, L. Ma, Y. Wang, et al., Chin. Chem. Lett. 36 (2025) 109766.
[14] S. Setua, S. Shabir, P. Shaji, et al., Acta Pharm. Sin. B 14 (2024) 3009–3026.
[15] P. Yu, Y. Han, L. Meng, et al., Acta Pharm. Sin. B 14 (2024) 2039–2056.
[16] W. Chi, Y. He, S. Chen, et al., Acta Pharm. Sin. B 15 (2025) 3511–3544.
[17] H. Peng, W. Ji, R. Zhao, et al., J. Mater. Chem. B 8 (2020) 7591–7608.
[18] H. Fu, Y. Chen, Q. Fu, et al., Chem. Eng. J. 500 (2024) 156685.
[19] Y. Yu, H. Zhou, Y. Xiong, et al., Brain Res. 1726 (2020) 146515.
[20] L. Li, J. Mu, Y. Zhang, et al., ACS Nano 16 (2022) 10811–10823.
[21] P. Cheng, X. Xie, L. Hu, et al., Bioact. Mater. 33 (2024) 157–173.
[22] M. Rizzuti, M. Nizzardo, C. Zanetta, et al., Drug Discov. Today 20 (2015) 76–85.
[23] H. Wu, Y. Wang, Z. Ren, et al., Chin. Chem. Lett. 36 (2025) 109996.
[24] S.V. Dhuria, L.R. Hanson, W.H. Frey, J. Pharm. Sci. 99 (2010) 1654–1673.
[25] N.C. Fernandes, U. Sriram, L. Gofman, et al., J. Neuroinflammation 13 (2016) 91.
[26] T. Kanazawa, F. Akiyama, S. Kakizaki, et al., Biomaterials 34 (2013) 9220–9226.
[27] L. Qiao, Y. Qin, Y. Wang, et al., RSC Adv. 10 (2020) 41471–41481.
[28] S. Hernando, E. Herran, J. Figueiro-Silva, et al., Mol. Neurobiol. 55 (2018) 145–155.
[29] T. Kanazawa, H. Taki, K. Tanaka, et al., Pharm. Res. 28 (2011) 2130–2139.